
Exploring Semantic Clustering in Deep Reinforcement Learning for Video Games

Liang Zhang*

School of Information
University of Arizona
Tucson, AZ, USA
liangzh@arizona.edu

Justin Lieffers

School of Information
University of Arizona
Tucson, AZ, USA
lieffers@arizona.edu

Adarsh Pyarelal

School of Information
University of Arizona
Tucson, AZ, USA
adarsh@arizona.edu

Abstract

In this paper, we investigate the semantic clustering properties of deep reinforcement learning (DRL) for video games, enriching our understanding of the internal dynamics of DRL and advancing its interpretability. In this context, semantic clustering refers to the inherent capacity of neural networks to internally group video inputs based on semantic similarity. To achieve this, we propose a novel DRL architecture that integrates a semantic clustering module featuring both feature dimensionality reduction and online clustering. This module seamlessly integrates into the DRL training pipeline, addressing instability issues observed in previous t-SNE-based analysis methods and eliminating the necessity for extensive manual annotation of semantic analysis. Through experiments, we validate the effectiveness of the proposed module and the semantic clustering properties in DRL for video games. Additionally, based on these properties, we introduce new analytical methods to help understand the hierarchical structure of policies and the semantic distribution within the feature space.

1 Introduction

Human beings excel at summarizing and categorizing knowledge from complex tasks with large amounts of information, enabling rapid skill acquisition for better adaptation to their environment [1–3]. Some applications of neural networks that simulate the human brain, have revealed semantic clustering properties. We use the term *semantic clustering* to refer to a neural network’s intrinsic ability to internally organize information based on semantic similarity. For example, in natural language processing (NLP), the spatial arrangement of word embeddings [4, 5] mirrors semantic similarities between words, resulting in clusters of semantically related words in the embedding space. In computer vision (CV), semantic clustering denotes neural networks’ intrinsic ability to organize visual information based on semantic similarity, improving efficiency in tasks such as image classification, clustering, segmentation [6–9].

While semantic clustering has been extensively explored in NLP and CV, our understanding of its implications in deep reinforcement learning (DRL) remains limited. This is primarily due to the complexity of DRL, characterized by its temporal dynamics and lack of direct guiding signals from supervised learning. The interplay of sequential decisions over time presents a challenge in capturing the evolving semantics within the framework of DRL. Early efforts in this domain sought to introduce *external* constraints, e.g., bisimulation [10, 11] and contrastive learning [12–14], to construct feature spaces with distributions conducive to semantic clustering. In contrast to these works, we investigate whether DRL *inherently* possesses the capacity to perform semantic clustering.

*Use footnote for providing further information about author (webpage, alternative address)—*not* for acknowledging funding agencies.

Mnih et al. [15] and Zahavy et al. [16] analyzed the semantic distribution of the feature space of DRL in Atari games based on the visualizations using t-distributed Stochastic Neighbor Embedding (t-SNE) [17]. However, these studies have certain limitations: (i) they are confined to a few Atari games with fixed scenes, making it challenging to discern whether clustering was due to pixel similarity or semantic understanding, (ii) Zahavy et al. [16] manually define features for specific games, limiting the adaptability of their method to other environments, and (iii) both use t-SNE for semantic analysis, which produces unstable results and lacks an automated mechanism for feature clustering. Thus, such approaches require significant manual effort for annotating and analyzing a subset of the feature space, preventing a comprehensive semantic analysis in DRL.

We use Procgen [18] as our testbed. With its rich semantics and dynamic, procedurally generated environments, Procgen is well-suited to our investigation into semantic clustering in DRL for video games. Specifically, we will study the following environments from Procgen: *CoinRun*, *Ninja*, *Fruitbot*, and *Jumper*.

In this paper, we make the following main contributions.

- We conduct an in-depth exploration of the semantic clustering properties of DRL in video games. This investigation enhances our understanding of the black-box decision-making processes within DRL.
- We introduce a novel architecture that addresses the limitations in previous semantic analysis methods based on t-SNE, providing a more robust and effective approach for studying semantic properties in DRL.
- Based on our experimental results, we present new methods for model and policy analysis. These approaches aid in comprehending the internal semantic distribution, understanding the hierarchical structure of policies, and identifying potential risks in DRL.

2 Related Work

Semantic Clustering in NLP and CV Prior work has demonstrated that the spatial configuration of word embeddings reflects semantic similarities among words, resulting in the formation of clusters containing semantically related terms in the embedding space [4, 5]. Similarly, in CV, semantic clustering characterizes the inherent capability of neural networks to structure visual information based on semantic similarity. This process demonstrates that images sharing semantic content are proximal in the learned feature space. The intrinsic semantic structure in visual data supports improved performance in CV tasks, e.g., image classification, clustering, and segmentation [6–9].

Semantic Clustering in DRL The use of t-SNE for visualizing the feature space in DRL has been previously explored by Mnih et al. [15] and Zahavy et al. [16]. t-SNE methods transform the distance metric between data points into conditional probabilities in both the original high-dimensional and mapped low-dimensional spaces. The optimization process involves minimizing the Kullback-Leibler divergence between these probabilities. The t-SNE visualizations in these studies, driven by RL policy training for dimensionality reduction in the feature space, reveal that features of states with close pixel distances tend to cluster together. However, due to the fixed nature of the tested Atari game scenarios, the existence of semantic clustering could not be effectively verified. This observation motivates our usage of Procgen to validate our approach, since it supports the generation of varied environments that are nevertheless semantically similar.

Interpretability of DRL Many studies have contributed to enhancing the interpretability of DRL. Approaches such as attention mechanisms generate attention maps for individual frames to elucidate the agent’s decision-making focus [19, 20]. The Symbolic Deep Reinforcement Learning (SDRL) framework [21] explicitly represents symbolic knowledge for high-level symbolic planning, incorporating intrinsic goals, and uses DRL for learning low-level control policies, thereby improving task-level interpretability. Linear Model U-trees (LMUTs) [22] approximate neural network predictions with expressive power suitable for approximating a Q-value function. Other works have explored diverse visualization methods to enhance RL interpretability [16, 23, 24]. Unlike the aforementioned works, we focus on understanding how DRL models internally group information, providing insights into the spatial structure of the learned representations.

3 Method

The proposed architecture with a novel semantic clustering module is presented in Figure 1.

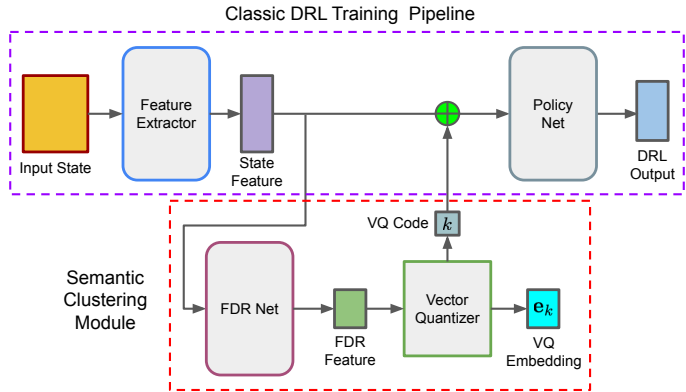


Figure 1: Overview of our architecture. The upper segment represents the classic DRL training pipeline, while the lower segment introduces the semantic clustering module. The Feature Dimensionality Reduction (FDR) net reduces the dimensionality of state features, resulting in FDR features, which the vector quantizer then processes to generate discrete VQ codes (denoted k), which represent states associated with clusters, along with the closest VQ embeddings. Subsequently, k is integrated into the state feature after expansion into a vector with the same dimensions as the state feature.

Background Vector-quantized variational autoencoders (VQ-VAE) [25] comprise a successful family of generative models that combine the variational autoencoder (VAE) framework with discrete latent representations through a novel parameterization of the posterior distribution. The VQ-VAE workflow starts with an encoder network \hat{E} that maps an input \mathbf{x} to a latent representation $\hat{E}(\mathbf{x})$. This representation is then quantized by mapping it to the nearest embedding in a codebook $\{\mathbf{e}_1, \dots, \mathbf{e}_K\}$, where \mathbf{e}_i is the i^{th} embedding in the codebook and K is the number of embeddings in the codebook. This nearest neighbor embedding is then fed into a decoder network \hat{D} to reconstruct the input \mathbf{x} . The loss function for VQ-VAE is given by

$$\mathcal{L}_{\text{VQ-VAE}} = \|\mathbf{x} - \hat{D}(\mathbf{e})\|_2^2 + \|sg[\hat{E}(\mathbf{x})] - \mathbf{e}\|_2^2 + \beta \|sg[\mathbf{e}] - \hat{E}(\mathbf{x})\|_2^2, \quad (1)$$

where sg is a stop-gradient operator and β weights the distance reduction between the encoded output $\hat{E}(\mathbf{x})$ and its closest embedding \mathbf{e}_k .

3.1 Semantic Clustering Module

Inspired by the findings of Mnih et al. [15] and Zahavy et al. [16], we hypothesize the presence of semantic clustering properties in DRL models for Procgen’s environments, facilitating the clustering of features based on their mutual proximity. Furthermore, to address limitations identified in the previous t-SNE-based semantic analysis (see § 1), we introduce a novel semantic clustering module.

Dimensionality Reduction Considering the complexity of video game states, their features are frequently high-dimensional; e.g., DQN [15] requires 512-dimensional features when trained on Atari games. Since it is challenging to cluster high-dimensional features directly, we propose to reduce the dimensionality of video game features and ensure the *distance relationship* between features in high- and low-dimensional spaces as much as possible (measured by pairwise similarities in § 3.2), which is functionally similar to the idea of t-SNE used in [15, 16]. Dimensionality reduction can also show the feature distribution in a human-interpretable manner, usually by visualizing it in a 2D space.

To mitigate the limitations of t-SNE techniques, we propose the *Feature Dimensionality Reduction* (FDR) network. This network remaps high-dimensional features to 2D, using policy training data for online training, ensuring stable and quick mapping post-training. As detailed in § 3.2, the FDR network’s loss function is designed to maintain the consistency of feature distance relationships between high-dimensional and 2D spaces.

Online Clustering Unlike implementing the discrete encoding of features based on reconstruction tasks in previous VQ-VAE applications [26–28], we propose a modified VQ-VAE to achieve online clustering. VQ-VAE clusters the surrounding features centered on the VQ embeddings in its codebook, used to discretely encode features online. Training a VQ-VAE model is functionally similar to performing online clustering. Ideally, the clustering based on VQ-VAE should not affect feature locations. However, the original VQ-VAE causes VQ embeddings and nearby features to move towards each other, which does not align with our goal of preserving feature distance relationships between high- and low-dimensional spaces.

Additionally, since we aim to perform online clustering using VQ-VAE, the state reconstruction based on VQ embeddings is not required. Therefore, we modify the VQ-VAE loss (see § 3.2). Our modified VQ-VAE procedure segments the feature space into clusters by identifying the closest VQ embedding to the feature and returning its corresponding index in the codebook.

3.2 Loss Function Design

The loss function for our proposed framework is given by

$$\mathcal{L}_{\text{total}} = \mathcal{L}_{\text{DRL}} + f_{\text{control}} \left(w_{\text{FDR}} \mathcal{L}_{\text{FDR}} + w_{\text{VQ-VAE}} \mathcal{L}'_{\text{VQ-VAE}} \right). \quad (2)$$

The DRL loss function \mathcal{L}_{DRL} comes from the original DRL model without any changes. w_{FDR} and $w_{\text{VQ-VAE}}$ are the weights of the FDR loss (\mathcal{L}_{FDR}) and the modified VQ-VAE loss ($\mathcal{L}'_{\text{VQ-VAE}}$), respectively.

FDR Loss The FDR loss function is based on the state features in the training batch and the FDR features mapped with the FDR net. Our goal is to keep the conditional probabilities of features in low-dimensional space as consistent as possible with those in high-dimensional space to ensure the accuracy of our distance-based clustering. The Student’s t-distribution with a high degree of freedom can approximate a Gaussian distribution, thus avoiding tuning and estimating other parameters for the Gaussian distribution [29]. For this reason, we use it to measure the pairwise similarities of state features p_{ij} in the two spaces, given by

$$p_{ij} = \frac{d(i, j)}{\sum_{k \neq l} d(k, l)}, \text{ where } d(m, n) = \left(1 + \|f(\mathbf{s}_m) - f(\mathbf{s}_n)\|^2 / \alpha \right)^{-\frac{\alpha+1}{2}} \quad (3)$$

where f is the feature extractor, \mathbf{s} is a state in a batch, and α is the degree of freedom of the Student’s t-distribution. The pairwise similarities for FDR features, q_{ij} are computed using the same expression as (3), but with f replaced by $g \circ f$, where g is the FDR net. In contrast to other deep clustering studies, e.g., Xie et al. [30] and Li et al. [31], the same degree of freedom α is selected for both high- and low-dimensional similarities, ensuring that the original distance relationship between features is maintained as much as possible in the low-dimensional space.

Furthermore, rather than using traditional clustering methods (e.g., k -means), we perform VQ encoding online for clustering based on the preserved distance relationship of features in the low-dimensional space. The FDR loss is given by

$$\mathcal{L}_{\text{FDR}} = - \sum_i \sum_j p_{ij} \log(q_{ij}). \quad (4)$$

Modified VQ-VAE Loss The first term in $\mathcal{L}_{\text{VQ-VAE}}$ from (1) supports input reconstruction, which our model does not need. The third term causes FDR features to align with their nearest VQ embeddings, while the second term moves VQ embeddings closer to adjacent FDR features. Therefore, we eliminate the first and third terms and modify the second term to obtain the modified VQ-VAE loss:

$$\mathcal{L}'_{\text{VQ-VAE}} = \|sg[g(f(\mathbf{s}))] - \mathbf{e}\|_2^2, \quad (5)$$

where \mathbf{e} is the closest embedding in the codebook to the FDR feature $g(f(\mathbf{s}))$.

Control Factor Since effective semantic clustering relies on a clear and distinguishable semantic distribution that is often difficult to achieve in the early stage of training, we propose an adaptive control factor strategy updated according to training performance, see Appendix A. f_{control} in (2) represents the control factor.

Improved Semantic Clustering Although sg in \mathcal{L}'_{VQ-VAE} prevents FDR features from moving to the closest VQ embeddings, when FDR features under the influence of \mathcal{L}_{FDR} are denser, it will indirectly reduce \mathcal{L}'_{VQ-VAE} and thus reduce \mathcal{L}_{total} . In other words, training jointly with \mathcal{L}_{FDR} and \mathcal{L}'_{VQ-VAE} decreases the sum of the distances between the FDR features in the same cluster and their VQ embedding. In addition, since \mathcal{L}_{FDR} needs to make p and q closer, this improved cluster density from the FDR feature space is also transferred to the state feature space. We will demonstrate the improved semantic clustering in § 4.

Advantages of Online Training Online training presents several advantages. (i) It enhances semantic clustering by incorporating the training of \mathcal{L}_{total} , facilitating the semantic differentiation of features along cluster boundaries. This distinction is crucial for making the semantics between clusters more discernible, enabling a clearer semantic analysis and enhancing the interpretability of models and policies. (ii) Training the VQ code k with a latent-conditioned policy $\pi(a|s, k)$ (where a is the action) potentially contributes to the extension of downstream tasks, such as the macro action selection in hierarchical learning. (iii) Online training improves the memory efficiency of model training by obviating the need for additional memory to store numerous states.

The training process of the proposed framework follows the structure of the original DRL algorithm, except using (2) when calculating the total loss.

4 Simulations

In this section, we aim to: 1) validate the clustering effectiveness of our proposed method, 2) assess the semantic clustering properties of DRL for video games, and 3) introduce new methods for policy and model analysis.

4.1 Assessing Clustering Effectiveness

We illustrate the clustering effectiveness of our proposed approach using CoinRun as an example. A similar conclusion can be easily extended to other games by using the code and checkpoints in the supplementary material. We employ a trained model to collect states, using a strategy where the agent randomly selects an action with probability 0.2 while following the trained policy with probability 0.8 to ensure diverse state coverage. States are collected with probability 0.8, and 64 parallel environments gather states for 500 steps, resulting in the collection of nearly 25,000 states for visualization.

Cluster Separation The t-SNE visualization of PPO (Figure 2a), spreads features across the space without forming clear clusters, limiting its utility for clustering analysis and requiring detailed manual examination of certain areas, as in previous studies. In contrast, the t-SNE visualization of our method (Figure 2b), reveals numerous distinct, small clusters. States within each of these clusters originate from the same semantic group identified by our method. This dispersion into multiple smaller clusters is due to t-SNE’s focus on local structures and its tendency to avoid crowding, causing complete semantic clusters to scatter. The visualization in the FDR space (Figure 2d), displays clear and separate complete clusters, which are identified by VQ codes.

Sensitivity to Number of States Our method’s stability is showcased in Figures 2c and 2e, where the number of processed states is reduced by 50%. Unlike the drastic changes in feature distribution seen in the t-SNE space (Figure 2c), the FDR space (Figure 2e) exhibits a stable mapping, merely reducing the quantity of features without altering their spatial distribution.

Sensitivity to Random Seed While the t-SNE representation is sensitive to randomness, as demonstrated by the significant difference between Figures 2c and 2f, the FDR space’s mapping remains unchanged even when the random seed is altered, maintaining a consistent distribution as in Figure 2e. t-SNE’s randomness primarily stems from its random initialization and non-convex optimization process, leading to different visualizations with different random seeds. In contrast, our model produces a stable feature mapping after training, which does not vary with random seeds.

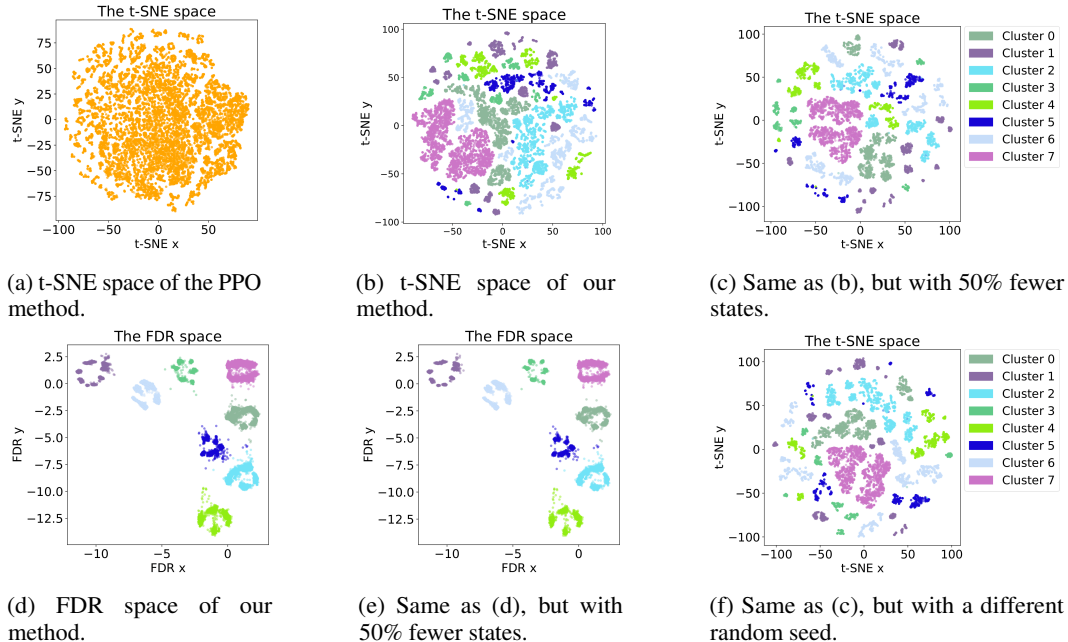


Figure 2: Visualization of features in t-SNE and FDR spaces, using PPO and our method. To facilitate comparing spatial relationships and changes in feature distributions, feature colors in the t-SNE visualizations of our method correspond to the cluster colors in the FDR space. Note that PPO-generated features are uniformly colored orange as they lack cluster information.

These stark contrasts underscore the FDR space’s mapping robustness compared to t-SNE’s instability, addressing the limitations of previous t-SNE-based analysis methods and laying a solid foundation for stable semantic clustering analysis and our proposed policy and model analysis.

4.2 Semantic Clustering in DRL

In this section, we illustrate semantic clustering analysis using the Ninja game. In the Ninja game, the agent navigates from the leftmost to the rightmost part of the scene, jumping over various ledges and scoring points by touching the mushroom on the far right. In the appendix, we analyze additional games, reaching similar conclusions.

Mean Image Analysis We performed a qualitative analysis of the mean images of states within each cluster. Figure 3 presents state examples from the FDR space of Ninja, along with the mean images of each semantic cluster, and Table 1 contains natural language descriptions of the clusters as well as notable features of the mean images corresponding to each cluster. Corresponding videos can be found in the supplementary material.

Unlike *static* semantic clustering in some CV and NLP tasks, where clustering is based on a single image or word, DRL’s semantic clustering is *dynamic* in nature—state sequences with similar semantics are grouped into the same semantic cluster. Notably, this semantic clustering goes beyond pixel distances and operates on a *semantic understanding* level of the environment, as illustrated in figures 3 and 4. This generalized semantic clustering emerges from the DRL model’s inherent ability to learn and summarize from changing scene dynamics, independent of external constraints like bisimulation or contrastive learning, and without the need for supervised signals. The neural network’s internal organization of policy-relevant knowledge indicates clustering-based spatial organization based on semantic similarity. Furthermore, we find that video sequences within clusters can be summarized using natural language, akin to the ‘*skills*’ humans abstract during learning processes.

Human Evaluation In addition to qualitatively analyzing the mean images, we hired 15 human evaluators to validate the semantic clustering properties. Specifically, video sequences from each episode are segmented into multiple clips based on the cluster each frame belongs to, and these clips

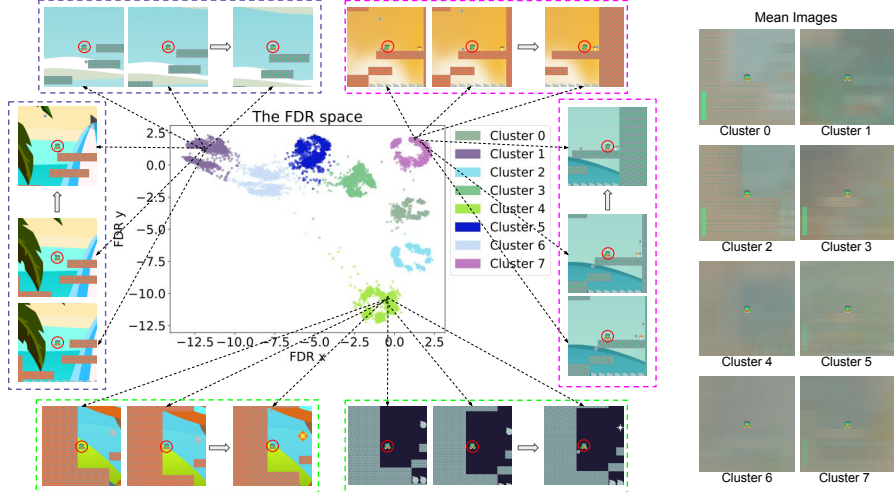


Figure 3: State examples in the Ninja FDR space and the mean images of clusters. Each dashed box contains a set of consecutive states from the same cluster. The dotted arrows indicate the positions of the FDR features corresponding to the states. Descriptions of the state sequences in the clusters are provided in Table 1.

are grouped by cluster for evaluators to review. Each evaluator watched these grouped clips and responded to three statements regarding interpretability for two out of a set of three games (Jumper, Fruitbot, and Ninja) The response for each question was chosen from a five-point Likert scale with the following options: *Strongly Disagree* (1), *Disagree* (2), *Neutral* (3), *Agree* (4), and *Strongly Agree* (5). More details on the human evaluation procedure are provided in Appendix F. The statements and the results of the human evaluation are provided in Table 2. The mean scores for each statement are all greater than 4 for each statement-environment combination, with the exception of statements 1 and 3 for FruitBot, for which the lower bounds on the mean set by the standard error of the mean are 3.99 and 3.92 respectively. One explanation for the slightly lower score on FruitBot is that in the description of behaviors within clusters in FruitBot, the agent’s relative distance to the wall ahead (far/near) and the agent’s relative position on the screen (left/center/right) require a certain degree of subjective judgment—in contrast, Jumper has a clear radar for direction and position information, and Ninja has more explicit behavioral reference objects, e.g., ledges and mushrooms. These results suggest that humans generally agree that our model possesses semantic clustering properties and supports interpretability.

4.3 Model and Policy Analysis

To better explore the knowledge organization within the internal space of DRL models, we developed a visualization tool (see Figure 5 for an example). The tool supports ‘statically’ analyzing the semantic distribution of models—specifically, (i) when the mouse cursor hovers over a specific feature point, the corresponding state image is displayed, and (ii) the tool includes a zooming functionality to observe the semantic distribution of features in detail within clusters.

In addition, we propose a more ‘dynamic’ analysis method—the VQ code enables us to determine the cluster to which the current state belongs, which allows for the semantic segmentation of episodes, as exemplified in Figure 4. Our model excels at breaking down complex policies, thereby shedding light on their inherent hierarchical structures. Moreover, this segmentation is based on semantics, making it understandable to humans and likely to improve interpretability in downstream hierarchical learning tasks. Consequently, this method introduces a ‘dynamic’ strategy for dissecting policy structures.

We also present several examples of policy analysis in Figure 6, based on the clustering result from our approach. In 6(a) and 6(b), two consecutive states are shown, with 6(a) and 6(b) belonging to clusters 5 and 7 respectively. We see that determining whether the agent will exhibit the behavior of approaching the mushroom does not depend on the appearance of the mushroom, but rather on the presence of the right-side wall. This is validated in another episode shown in 6(c), which belongs to

Table 1: Cluster descriptions and mean image outlines for the Ninja game

Cluster	Description	Mean image outlines
0	The agent starts by walking through the first platform and then performs a high jump to reach a higher ledge.	Essential elements are outlined, e.g., a left-side wall, the current position of the agent on the first platform, and the upcoming higher ledges.
1	The agent makes small jumps in the middle of the scene.	We can observe the outlines of several ledges below the agent.
2	Two interpretations are present: 1) the agent starts from the leftmost end of the scene and walks to the starting position of Cluster 0, and 2) when there are no higher ledges to jump to, the agent begins from the scene, walks over the first platform, and prepares to jump to the subsequent ledge.	The scene prominently displays the distinct outline of the left wall and the first platform. The agent’s current position is close to both of them.
3	The agent walks on the ledge and prepares to jump to a higher ledge.	The agent is standing on the outline of the current ledge and the following higher ledges.
4	After performing a high jump, the agent loses sight of the ledge below.	The agent can be observed performing a high jump.
5	The agent walks on the ledge and prepares to jump onto a ledge at the same height or lower.	The agent is standing on the outline of the current ledge and the following ledges at the same height or lower.
6	The agent executes a high jump while keeping the ledge below in sight.	The agent is performing a high jump and the outline of the ledge below is visible.
7	The agent moves towards the right edge of the scene and touches the mushroom.	The outlines of the wall and platform on the far right are visible.

Table 2: Human evaluation results (mean score \pm standard error of the mean (SEM))

No.	Stmt. Wording	Jumper	FruitBot	Ninja
1	<i>The clips of each cluster consistently display the same skill being performed</i>	4.24 \pm 0.15	4.10 \pm 0.11	4.30 \pm 0.15
2	<i>The clips of each cluster match the given skill description</i>	4.36 \pm 0.16	4.16 \pm 0.11	4.20 \pm 0.17
3	<i>The identified skills aid in understanding the environment and the AI’s decision-making process</i>	4.50 \pm 0.22	4.10 \pm 0.18	4.20 \pm 0.20

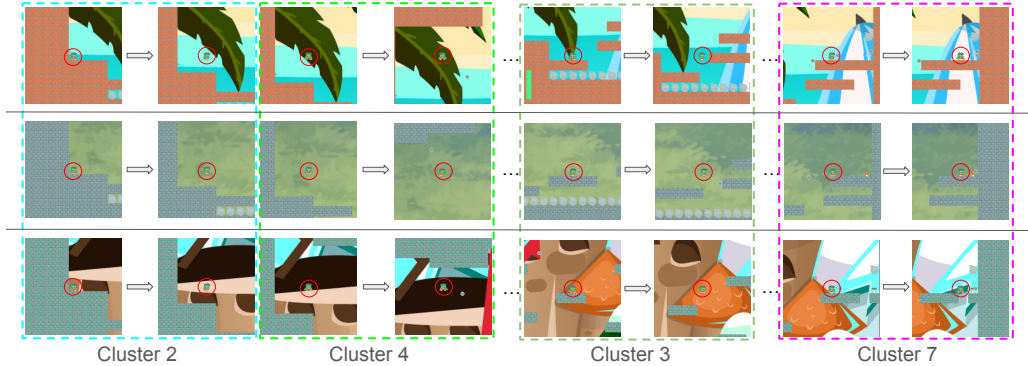


Figure 4: Three episodes from the Ninja game. States within colored dashed boxes correspond to the clusters of the same colors in Figure 3. Solid gray arrows indicate omitted states from the same cluster. Ellipses represent other omitted states.

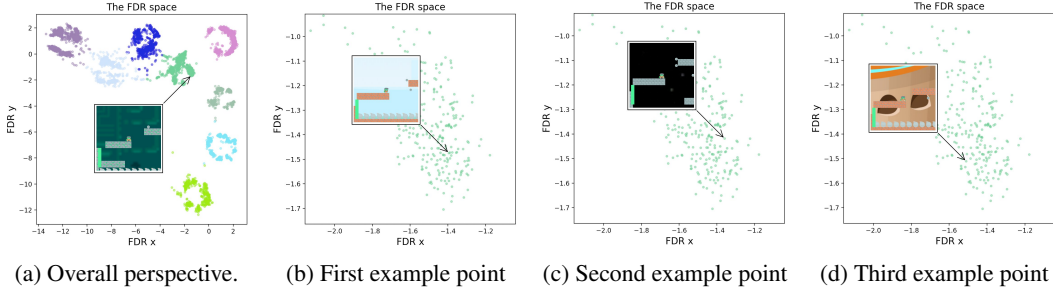


Figure 5: Hover examples in the FDR space of Ninja. We observe a sub-cluster in the FDR space as an example from the overall perspective (a) and the zoomed-in perspective (b), (c), and (d). The agent is standing on the edge of a ledge. Although the scenarios of (b), (c), and (d) are different, the proposed method effectively clusters semantically consistent features together in the FDR space.

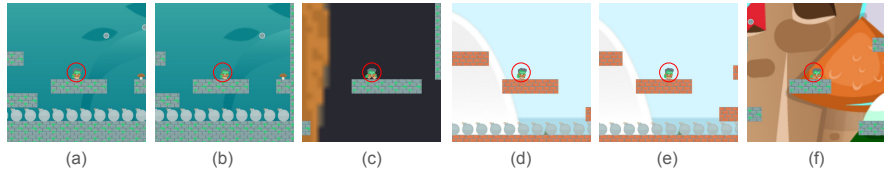


Figure 6: Policy analysis examples in Ninja.

cluster 7 but lacks the appearance of a mushroom. The agent goes back and forth on the ledge for an extended period, consistently remaining in cluster 7, as it mistakenly interprets the key condition for executing behaviors in cluster 7. 6(d) and 6(e) show two states in the same episode. In 6(d), before a higher ledge comes into view, the agent anticipates jumping onto a lower ledge ahead (i.e., the behavior in cluster 5). However, when the higher ledge appears in 6(e), it adjusts its strategy, opting to jump onto the (safer) higher ledge—i.e., executing the behavior in cluster 3. Similarly, 6(f) shows a state that has been assigned to cluster 3 by our model, helping us anticipate the agent’s future behavior of jumping onto the higher ledge. These analyses based on our proposed model contribute to a better understanding of policies, revealing underlying structures and identifying issues.

5 Limitations and Future Work

Our approach has a few known limitations, which we aim to address in future work. First, semantic clustering depends on clear semantic distributions in the FDR space, posing challenges when policies deviate significantly from the optimum, resulting in chaotic semantic distributions. Second, as approach uses unsupervised learning, the selection of the number of clusters is crucial; we opted for eight clusters to predominantly ensure a singular semantic interpretation, although a few clusters might encompass up to two interpretations. Finally, we will extend our exploration to additional DRL algorithms, benchmarks, and practical applications.

6 Conclusion

In this paper, we investigated the semantic clustering properties of DRL for video games. Using a novel approach that combines dimensionality reduction and online clustering, we analyzed the internal organization of knowledge within the feature space of a DRL model (PPO). Our method not only provides a stable mapping of feature positions but also enhances semantic clustering, revealing meaningful structures within continuous sequences of video game states. We show that in DRL, the dynamic nature of semantic clustering arises organically through the agent’s interaction with its environment. As the agent explores diverse states during reinforcement learning, it naturally clusters semantically related states based on spatial and temporal relationships within the environment. This dynamic clustering is a result of the agent’s ability to exploit regularities, showcasing a distinctive approach compared to static semantic clustering approaches common in natural language processing and computer vision.

References

- [1] Scott T Grafton and Antonia F de C Hamilton. Evidence for a distributed hierarchy of action representation in the brain. In: *Human movement science* 26.4 (2007), pp. 590–616.
- [2] Brenden M Lake et al. Building machines that learn and think like people. In: *Behavioral and brain sciences* 40 (2017), e253.
- [3] Andrea Banino et al. Vector-based navigation using grid-like representations in artificial agents. In: *Nature* 557.7705 (2018), pp. 429–433.
- [4] Xin Rong. [word2vec Parameter Learning Explained](#). In: *CoRR* abs/1411.2738 (2014).
- [5] Jeffrey Pennington, Richard Socher, and Christopher Manning. [GloVe: Global Vectors for Word Representation](#). In: *Proceedings of the 2014 Conference on Empirical Methods in Natural Language Processing (EMNLP)*. Ed. by Alessandro Moschitti, Bo Pang, and Walter Daelemans. Doha, Qatar: Association for Computational Linguistics, Oct. 2014, pp. 1532–1543.
- [6] Sungwon Park et al. [Improving Unsupervised Image Clustering With Robust Learning](#). In: *IEEE Conference on Computer Vision and Pattern Recognition, CVPR 2021, virtual, June 19-25, 2021*. Computer Vision Foundation / IEEE, 2021, pp. 12278–12287.
- [7] Xu Ji, Andrea Vedaldi, and João F. Henriques. [Invariant Information Clustering for Unsupervised Image Classification and Segmentation](#). In: *2019 IEEE/CVF International Conference on Computer Vision, ICCV 2019, Seoul, Korea (South), October 27 - November 2, 2019*. IEEE, 2019, pp. 9864–9873.
- [8] Jianwei Yang, Devi Parikh, and Dhruv Batra. [Joint Unsupervised Learning of Deep Representations and Image Clusters](#). In: *2016 IEEE Conference on Computer Vision and Pattern Recognition, CVPR 2016, Las Vegas, NV, USA, June 27-30, 2016*. IEEE Computer Society, 2016, pp. 5147–5156.
- [9] Lei Zhou and Weyufeng Wei. [DIC: Deep Image Clustering for Unsupervised Image Segmentation](#). In: *IEEE Access* 8 (2020), pp. 34481–34491.
- [10] Mete Kemertas and Tristan Aumentado-Armstrong. [Towards Robust Bisimulation Metric Learning](#). In: *Advances in Neural Information Processing Systems 34: Annual Conference on Neural Information Processing Systems 2021, NeurIPS 2021, December 6-14, 2021, virtual*. Ed. by Marc’Aurelio Ranzato et al. 2021, pp. 4764–4777.
- [11] Amy Zhang et al. [Learning Invariant Representations for Reinforcement Learning without Reconstruction](#). In: *9th International Conference on Learning Representations, ICLR 2021, Virtual Event, Austria, May 3-7, 2021*. OpenReview.net, 2021.
- [12] Michael Laskin, Aravind Srinivas, and Pieter Abbeel. [CURL: Contrastive Unsupervised Representations for Reinforcement Learning](#). In: *Proceedings of the 37th International Conference on Machine Learning, ICML 2020, 13-18 July 2020, Virtual Event*. Vol. 119. Proceedings of Machine Learning Research. PMLR, 2020, pp. 5639–5650.
- [13] Rishabh Agarwal et al. [Contrastive Behavioral Similarity Embeddings for Generalization in Reinforcement Learning](#). In: *9th International Conference on Learning Representations, ICLR 2021, Virtual Event, Austria, May 3-7, 2021*. OpenReview.net, 2021.
- [14] Benjamin Eysenbach et al. [Contrastive Learning as Goal-Conditioned Reinforcement Learning](#). In: *Advances in Neural Information Processing Systems 35: Annual Conference on Neural Information Processing Systems 2022, NeurIPS 2022, New Orleans, LA, USA, November 28 - December 9, 2022*. Ed. by Sanmi Koyejo et al. 2022.
- [15] Volodymyr Mnih et al. [Human-level control through deep reinforcement learning](#). In: *Nat.* 518.7540 (2015), pp. 529–533.
- [16] Tom Zahavy, Nir Ben-Zrihem, and Shie Mannor. [Graying the black box: Understanding DQNs](#). In: *Proceedings of the 33rd International Conference on Machine Learning, ICML 2016, New York City, NY, USA, June 19-24, 2016*. Ed. by Maria-Florina Balcan and Kilian Q. Weinberger. Vol. 48. JMLR Workshop and Conference Proceedings. JMLR.org, 2016, pp. 1899–1908.
- [17] Laurens van der Maaten and Geoffrey Hinton. [Visualizing Data using t-SNE](#). In: *Journal of Machine Learning Research* 9.86 (2008), pp. 2579–2605.
- [18] Karl Cobbe et al. [Leveraging Procedural Generation to Benchmark Reinforcement Learning](#). In: *Proceedings of Machine Learning Research* 119 (2020), pp. 2048–2056.
- [19] Alexander Mott et al. [Towards Interpretable Reinforcement Learning Using Attention Augmented Agents](#). In: *Advances in Neural Information Processing Systems 32: Annual Conference on Neural Information Processing Systems 2019, NeurIPS 2019, December 8-14, 2019, Vancouver, BC, Canada*. Ed. by Hanna M. Wallach et al. 2019, pp. 12329–12338.
- [20] Wenjie Shi et al. [Self-Supervised Discovering of Interpretable Features for Reinforcement Learning](#). In: *IEEE Transactions on Pattern Analysis and Machine Intelligence* 44.5 (2022), pp. 2712–2724.

- [21] Daoming Lyu et al. [SDRL: Interpretable and Data-Efficient Deep Reinforcement Learning Leveraging Symbolic Planning](#). In: *The Thirty-Third AAAI Conference on Artificial Intelligence, AAAI 2019, The Thirty-First Innovative Applications of Artificial Intelligence Conference, IAAI 2019, The Ninth AAAI Symposium on Educational Advances in Artificial Intelligence, EAAI 2019, Honolulu, Hawaii, USA, January 27 - February 1, 2019*. AAAI Press, 2019, pp. 2970–2977.
- [22] Guiliang Liu et al. [Toward Interpretable Deep Reinforcement Learning with Linear Model U-Trees](#). In: *Machine Learning and Knowledge Discovery in Databases - European Conference, ECML PKDD 2018, Dublin, Ireland, September 10-14, 2018, Proceedings, Part II*. Ed. by Michele Berlingerio et al. Vol. 11052. Lecture Notes in Computer Science. Springer, 2018, pp. 414–429.
- [23] Raghuram Mandyam Annasamy and Katia P. Sycara. [Towards Better Interpretability in Deep Q-Networks](#). In: *The Thirty-Third AAAI Conference on Artificial Intelligence, AAAI 2019, The Thirty-First Innovative Applications of Artificial Intelligence Conference, IAAI 2019, The Ninth AAAI Symposium on Educational Advances in Artificial Intelligence, EAAI 2019, Honolulu, Hawaii, USA, January 27 - February 1, 2019*. AAAI Press, 2019, pp. 4561–4569.
- [24] Jinyoung Choi, Beom-Jin Lee, and Byoung-Tak Zhang. [Multi-Focus Attention Network for Efficient Deep Reinforcement Learning](#). In: AAAI Technical Report WS-17 (2017).
- [25] Aäron van den Oord, Oriol Vinyals, and Koray Kavukcuoglu. [Neural Discrete Representation Learning](#). In: (2017). Ed. by Isabelle Guyon et al., pp. 6306–6315.
- [26] Ali Razavi, Aäron van den Oord, and Oriol Vinyals. [Generating Diverse High-Fidelity Images with VQ-VAE-2](#). In: *Advances in Neural Information Processing Systems 32: Annual Conference on Neural Information Processing Systems 2019, NeurIPS 2019, December 8-14, 2019, Vancouver, BC, Canada*. Ed. by Hanna M. Wallach et al. 2019, pp. 14837–14847.
- [27] Wilson Yan et al. [VideoGPT: Video Generation using VQ-VAE and Transformers](#). In: *CoRR* abs/2104.10157 (2021).
- [28] Cristina Gärbacea et al. [Low Bit-rate Speech Coding with VQ-VAE and a WaveNet Decoder](#). In: *IEEE International Conference on Acoustics, Speech and Signal Processing, ICASSP 2019, Brighton, United Kingdom, May 12-17, 2019*. IEEE, 2019, pp. 735–739.
- [29] Paras Dahal. [Learning Embedding Space for Clustering From Deep Representations](#). In: *IEEE International Conference on Big Data (IEEE BigData 2018), Seattle, WA, USA, December 10-13, 2018*. Ed. by Naoki Abe et al. IEEE, 2018, pp. 3747–3755.
- [30] Junyuan Xie, Ross B. Girshick, and Ali Farhadi. [Unsupervised Deep Embedding for Clustering Analysis](#). In: *Proceedings of the 33rd International Conference on Machine Learning, ICML 2016, New York City, NY, USA, June 19-24, 2016*. Ed. by Maria-Florina Balcan and Kilian Q. Weinberger. Vol. 48. JMLR Workshop and Conference Proceedings. JMLR.org, 2016, pp. 478–487.
- [31] Fengfu Li, Hong Qiao, and Bo Zhang. [Discriminatively boosted image clustering with fully convolutional auto-encoders](#). In: *Pattern Recognit.* 83 (2018), pp. 161–173.
- [32] Lasse Espeholt et al. [IMPALA: Scalable Distributed Deep-RL with Importance Weighted Actor-Learner Architectures](#). In: *Proceedings of the 35th International Conference on Machine Learning, ICML 2018, Stockholm, Sweden, July 10-15, 2018*. Ed. by Jennifer G. Dy and Andreas Krause. Vol. 80. Proceedings of Machine Learning Research. PMLR, 2018, pp. 1406–1415.
- [33] John Schulman et al. *Proximal Policy Optimization Algorithms*. 2017.

Appendix

Table of Contents

A Architecture, Hyperparameters, and Computational Costs	12
B Performance	12
C More Examples and Mean Images in the FDR Space	13
C.1 CoinRun	13
C.2 Jumper	13
C.3 FruitBot	15
D Hovering Examples	15
E Semantic Formation in Clusters	15
F Human Evaluation Details	16
F.1 Part 1: Overview and Timeline Introduction	16
F.2 Part 2: Questionnaire	17
F.3 Part 3: Evaluation Questions for Clarity Assessment	18
F.4 Part 4: Evaluation Questions for Interpretability Assessment	18
F.5 Part 5: Personnel and Coordination	18
F.6 Part 6: Grouping Details	19
G Potential Negative Societal Impacts	19

A Architecture, Hyperparameters, and Computational Costs

The training of the proposed method is consistent with the Impala architecture [32], the PPO algorithm [33], and hyperparameters used in the Procgen paper [18]. For more details, please refer to Section 2.3 and Appendix D in the Procgen paper. The FDR net is composed of two fully connected layers with 128 and 2 neurons, respectively. The codebook in the vector quantizer has eight embeddings, and the degree of freedom in the FDR loss is 20. The random seeds employed in Figure 2 are 2021 and 2031, while the seeds used in Figure B.1 are 2021, 2022, and 2023. We train all models on one NVIDIA Tesla V100S 32GB GPU. The operating system version is CentOS Linux release 7.9.2009.

In Equation 2 of the main paper, w_{FDR} and $w_{\text{VQ-VAE}}$ are 500 and 1, respectively. f_{control} is updated every 50 iterations according to the following expression:

$$f_{\text{control}} = \min(s_{\text{mean}} / (0.8 \cdot s_{\text{highest}}), 1), \quad (\text{A.1})$$

where s_{mean} is the mean score of the last 100 episodes in training, and s_{highest} is the highest score of the environment.

B Performance

Considering the cost of time and computational resources, we opt for training our model on the full distribution of levels in the ‘easy’ mode. In Figure B.1, a comparison of performance curves between the proposed method and the baseline is presented, where ‘SPPO’ denotes ‘semantic’ PPO, i.e., PPO integrated with our proposed semantic clustering module. Consistent with the Procgen paper [18], given the diversity of episodes during training, a single curve represents both training and testing

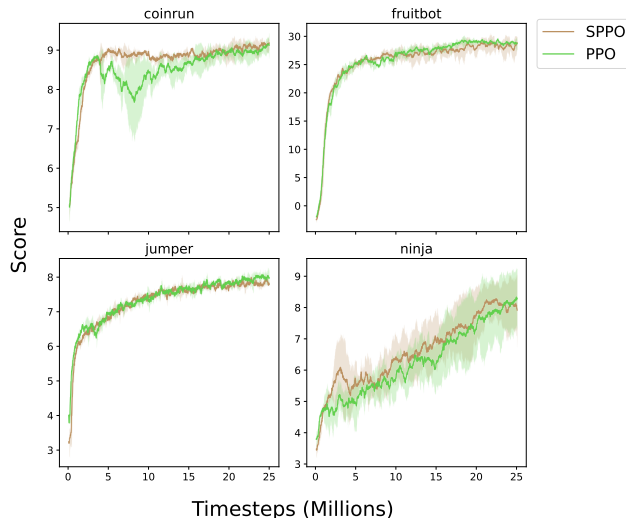


Figure B.1: Performance curves on ‘easy’ difficulty environments using three random seeds, trained and evaluated on the full distribution of levels.

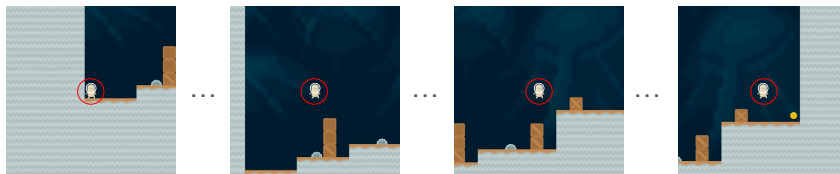


Figure C.1: A episode in CoinRun. Ellipses represent the omitted states.

performance. Across these environments we observe that the proposed method closely aligns with the baseline performance, indicating minimal impact on performance from the introduced module.

C More Examples and Mean Images in the FDR Space

C.1 CoinRun

To augment the exploration of semantic clustering as discussed in the main paper, this section analyzes two additional games characterized by distinct dynamics. CoinRun’s gameplay mechanism is similar to Ninja’s, requiring the agent to traverse from the far-left to the far-right, scoring points by interacting with coins at the far-right end of the scene, as illustrated in [Figure C.1](#).

The observations and insights obtained closely mirror those derived from the analysis of Ninja. Interested readers can leverage the provided code and checkpoint for further exploration of similar findings. Consequently, for brevity, we refrain from extensively elaborating on analogous conclusions.

C.2 Jumper

In Jumper, the agent navigates a cave to locate and touch carrots by interpreting a radar displayed in the upper right corner of the screen. The radar’s pointer indicates the direction of the carrot, while a bar below the radar shows the distance between the agent and the carrot—shorter bars imply closer proximity, and vice-versa.

The state examples and mean images from the clusters in the FDR space of Jumper are presented in [Figure C.2](#). The background of Jumper is diverse, and the agent is always in the center of the screen (zoom in to see the outlines clearly). In [Table 3](#), we break down descriptions of the sampled images from each cluster and interpretations of the mean image for each cluster in the Jumper game.

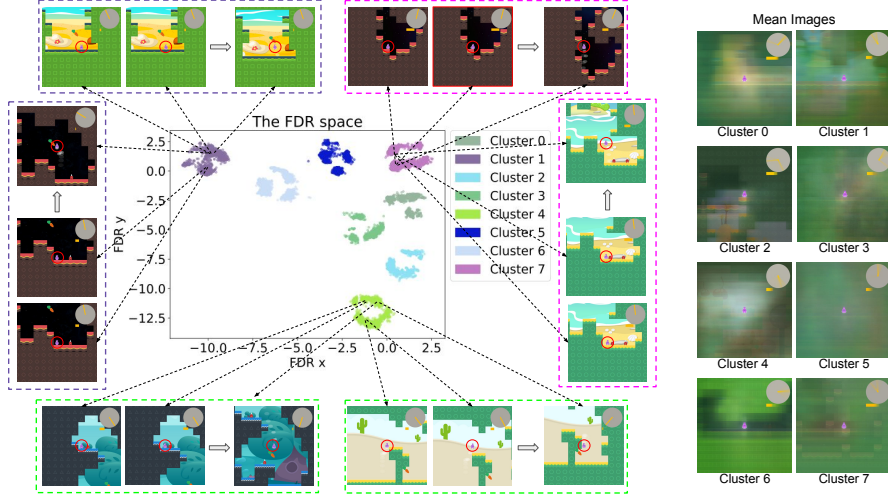


Figure C.2: Examples and mean images from the Jumper FDR space.

Table 3: Cluster descriptions and mean image outlines for the Jumper game

Cluster	Description	Mean image outlines
0	The agent learns to jump up from the bottom left and move to the left on the top right.	The radar pointing up and to the right, and the outline of the channel above and to the right..
1	The agent is touching the carrot on the left or upper left.	The radar is pointing to the upper left and is very close to the target.
2	The agent learns the skill of movement at the top of the scene.	The radar pointing to the left or down, and the outline of the channels face to the left or down.
3	The agent is approaching the carrot on the upper right.	The radar pointing to the upper right, and the distance to the target is very close.
4	The agent is touching the carrot below.	The radar is pointing down, and it is very close to the target.
5	The agent is approaching the carrot above or left.	The radar is pointing up, and it is very close to the target.
6	The agent is touching the carrot on the right.	The radar is pointing right, and it is very close to the target.
7	The agent learns the skill of movement at the right bottom of the scene.	The radar pointing up or to the top left, and it is far from the target.

Figure C.3 depicts various states from the Jumper game. C.3(a) and C.3(b) belong to the same episode and fall under Cluster 4, while C.3(c) and C.3(d) are from another episode, both categorized under Cluster 1. Notably, neither C.3(a) nor C.3(c) shows the presence of carrots. This observation leads us to suspect that the determination of these clusters is solely reliant on the radar and distance bar rather than the appearance of carrots. To test this hypothesis, we removed the carrot in C.3(e), which originally belonged to Cluster 4, and transformed it into C.3(f). The result demonstrated that C.3(f) still belongs to Cluster 4, confirming our suspicion. However, this phenomenon might pose potential risks in practical applications. For example, in scenarios where sensor data and visual perceptions misalign, AI models might solely rely on sensor data for decision-making—e.g., an autonomous vehicle’s sensors indicating an empty road while the occupants inside observe pedestrians crossing, yet the vehicle continues to accelerate.

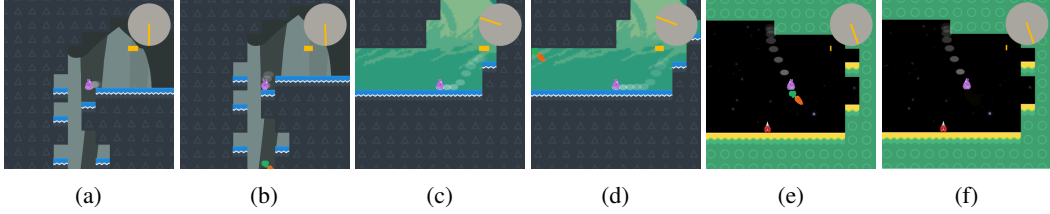


Figure C.3: Policy analysis examples in Jumper.

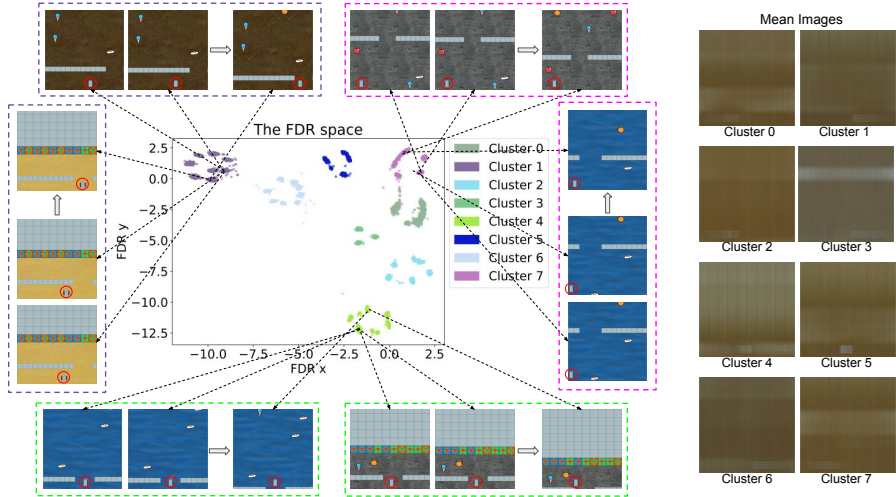


Figure C.4: State examples and mean images from the FruitBot FDR space.

C.3 FruitBot

FruitBot is a bottom-to-top scrolling game where the agent moves left or right to collect fruits for points while avoiding negative scores upon touching non-fruit objects. The state examples and mean images from the clusters in the FDR space of FruitBot are presented in Figure C.4 and their descriptions in Table 4. FruitBot’s mean images lack clarity due to the presence of diverse backgrounds, and the agent is constantly moving to the left and right at the bottom of the screen. However, we can still make out the outline of the wall and agent if we look carefully (zoom in to see the outlines clearly).

We examined a substantial number of video states and corresponding cluster information, and found that the factors determining clusters in FruitBot are the agent’s position on the screen and its relative positioning to walls and gaps. This suggests that the agent has learned critical factors within the environment.

D Hovering Examples

In figures D.1, and D.2, we present examples of our interactive visualization tool applied to Jumper and FruitBot. This tool is included in the supplementary material, allowing readers to freely explore the semantic distribution of features and gain a better understanding of the semantic clustering properties of DRL.

E Semantic Formation in Clusters

To provide insight into the generation of semantic clustering in the feature space, we conducted the statistical analysis as follows. Initially, we collected 50,000 states using the trained model and computed the mean image for each cluster. We then calculated the mean and standard deviation of

Table 4: Cluster descriptions and mean image outlines for the FruitBot game

Cluster	Description	Mean image outlines
0	The agent is approaching the wall in the left area.	We can see the agent moving toward the gap on the wall that is approaching on the lower left.
1	The agent approaches the wall from the right area.	The agent is moving toward the gap on the wall that is approaching on the lower right.
2	The agent executes its policy far from the wall from the left area.	The wall is far away, and the agent is moving in the lower left.
3	The agent approaches the wall from the right, but it is still some distance away.	The wall is far away, and the agent is moving in the lower right.
4	The agent is going through the gap in the middle and left, and insert the key at the end of the scene.	The agent going through the final gap and inserting the key.
5	The agent approaches the wall from the middle area.	We can identify the outline of the agent in the lower middle.
6	The agent going through the gap on the right, and performs policy far from the wall in the right area.	The agent is crossing the gap in the bottom right.
7	The agent approaches the wall from the left, but it is still some distance away.	The agent is moving in the lower left, and the outline of walls is in the middle of the screen.

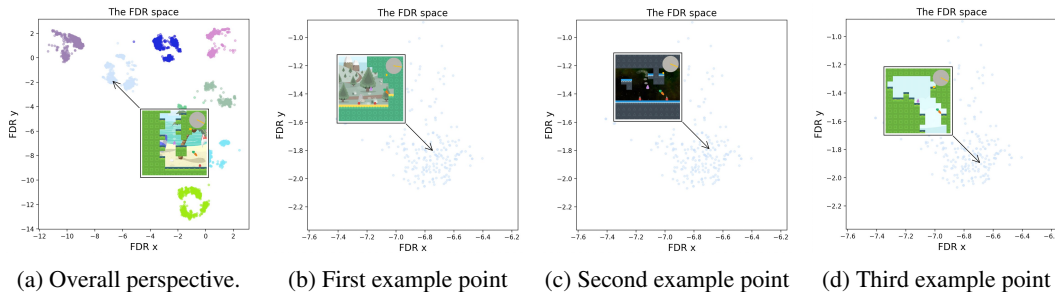


Figure D.1: Hover examples in the FDR space of Jumper. We observe a sub-cluster in the FDR space as an example from the overall perspective (a) and the zoomed-in perspective (b), (c), and (d). The agent is standing on the edge of a ledge. Although the scenarios of (b), (c), and (d) are different, the proposed method effectively clusters semantically consistent features together in the FDR space.

the pixel distances between the states in each cluster and their corresponding mean image. These measurements were averaged across the eight clusters. Additionally, we evaluated the probability of cluster transitions in these 50,000 states. We repeated the same statistical analysis on the 50,000 states using the untrained model, and the results are presented in Table 5. In the trained models, the pixel differences between the states within clusters increased, indicating the presence of states with similar semantics but larger pixel distances. Furthermore, the probability of cluster transitions decreased as it approached the required transition in the scene.

F Human Evaluation Details

F.1 Part 1: Overview and Timeline Introduction

This section provides a detailed description of the evaluation process and presents the timeline for conducting the assessment. The evaluation aims to assess the clarity and interpretability of the semantic clusters in the FruitBot, Jumper, and Ninja games, with the objective of enhancing and quantifying the explainability of the DRL system.

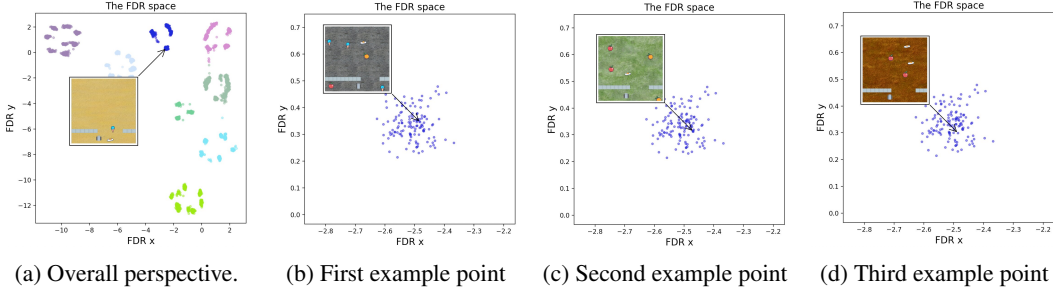


Figure D.2: Hover examples in the FDR space of Fruitbot. We observe a sub-cluster in the FDR space as an example from the overall perspective (a) and the zoomed-in perspective (b), (c), and (d). The agent is standing on the edge of a ledge. Although the scenarios of (b), (c), and (d) are different, the proposed method effectively clusters semantically consistent features together in the FDR space.

Table 5: Comparison metrics of the semantically trained model verse the raw model on various environments.

Model	Cluster transition probability	Pixel distance mean (Std. Dev.)
FruitBot Trained	0.1081	100.00 (71.33)
FruitBot Raw	0.2834	77.10 (49.94)
Jumper Trained	0.2224	110.29 (62.29)
Jumper Raw	0.5829	104.57 (58.31)
Ninja Trained	0.2680	141.50 (67.88)
Ninja Raw	0.2712	87.61 (62.43)

F.1.1 Timeline

Each participant will complete a survey for two game environments (FruitBot, Jumper, or Ninja). They follow the format as detailed:

- Stage 1: Questionnaire (5 minutes)**
 Participants are requested to complete a questionnaire that collects demographic information and gaming-related details. The questionnaire includes sections for gender, age group, education level, occupation, gaming experience, familiarity with evaluating game states, and preferred game genres.
- Stage 2: Introduction to Game Environment (10 minutes)**
 During this stage, participants receive an introduction to the evaluation process. They are informed about the objectives of the assessment and the significance of evaluating the clarity and interpretability of the semantic clusters. They are also given a short description of the game environment (FruitBot, Jumper, or Ninja), and are shown a short gameplay clip to aid with the understanding of the game’s objectives and features.
- Stage 3: Assessment (50 minutes)**
 Following the familiarization period, participants spend 50 minutes assessing the semantic clusters in the game environment. They focus on evaluating the clarity and understandability of the video clips within each semantic cluster. This is done online via a survey.

Total Evaluation Time: 60 minutes.

F.2 Part 2: Questionnaire

This section of the evaluation plan presents the questionnaire that participants are required to complete. The questionnaire consists of the following sections:

F.2.1 Demographic Information

- Age:** Participants indicate their age.

- **Gender:** Participants specify their gender as Male, Female, or Other.
- **Education Level:** Participants indicate their highest level of education completed, including options such as High school and below, Bachelor's degree, Master's degree, and Doctorate and above.
- **Occupation:** Participants provide their current occupation, selecting from options such as Student, Employee, Self-employed, or Other.

F.2.2 Gaming-related Information

- **Gaming Experience:** Participants indicate their level of gaming experience, choosing from options such as Beginner, Intermediate player, Advanced player, or Professional player.
- **Game Frequency:** Participants indicate their frequency of gaming, choosing from options such as Daily, Several times a week, Weekly, Monthly, or others.
- **Experience in Evaluating Game States:** Participants assess their experience in evaluating game states, selecting from options such as No experience, Some experience, Moderate experience, or Extensive experience.
- **Preferred Game Genres:** Participants specify their preferred game genres, including options such as Role-playing games, Shooting games, Strategy games, Puzzle games, or Other.

F.3 Part 3: Evaluation Questions for Clarity Assessment

In this section, a comprehensive set of questions is provided to assess the clarity and understandability of the semantic clusters. The questions capture participants' opinions and perceptions using a Likert scale ranging from 'Strongly Disagree' to 'Strongly Agree'. The specific evaluation questions for the clarity assessment include:

- The clips of each cluster consistently display the same skill being performed.
- The clips of each cluster match the given skill description.

The two questions are asked each time the participant has been shown a semantic cluster.

F.4 Part 4: Evaluation Questions for Interpretability Assessment

This section outlines the question evaluating the interpretability of the semantic clusters in terms of their usefulness. The question is designed to capture participants' opinions and perceptions using a Likert scale ranging from "Strongly Disagree" to "Strongly Agree." The specific evaluation question for the interpretability assessment:

- The identified skills aid in understanding the environment and the AI's decision-making process.

The above question is asked after the participants have seen all the semantic clusters.

F.5 Part 5: Personnel and Coordination

This section outlines the personnel and coordination aspects of the evaluation. It includes information about evaluator recruitment and compensation. Specifically:

F.5.1 Evaluator Recruitment

15 evaluators are recruited to participate in the evaluation.

F.5.2 Evaluator Compensation

Each evaluator receives \$15 in compensation for their valuable time and contribution to the evaluation process.

By implementing this comprehensive evaluation plan, we gather valuable insights into the clarity and interpretability of the semantic clusters in the FruitBot, Jumper, and Ninja games. The evaluation results provide essential guidance for further quantifying the improved interpretability of DRL models using our proposed method.

F.6 Part 6: Grouping Details

- **Evaluator 1:** FruitBot, Jumper
- **Evaluator 2:** FruitBot, Jumper
- **Evaluator 3:** FruitBot, Jumper
- **Evaluator 4:** FruitBot, Jumper
- **Evaluator 5:** FruitBot, Jumper
- **Evaluator 6:** Jumper, Ninja
- **Evaluator 7:** Jumper, Ninja
- **Evaluator 8:** Jumper, Ninja
- **Evaluator 9:** Jumper, Ninja
- **Evaluator 10:** Jumper, Ninja
- **Evaluator 11:** Ninja, FruitBot
- **Evaluator 12:** Ninja, FruitBot
- **Evaluator 13:** Ninja, FruitBot
- **Evaluator 14:** Ninja, FruitBot
- **Evaluator 15:** Ninja, FruitBot

This grouping plan ensures that each evaluator evaluates two different games, and each game receives a total of 10 evaluations. It allows for comprehensive evaluations of each game and ensures that evaluators have an opportunity to provide feedback on multiple games.

G Potential Negative Societal Impacts

As far as the authors are aware, there are currently no known potential negative societal impacts associated with this work.

